Energy Accumulation in a Functionally Graded Spatial-Temporal Checkerboard

Konstantin A. Lurie, Daniel Onofrei, William C. Sanguinet, Suzanne L. Weekes, and Vadim V. Yakovlev, *Senior Member, IEEE*

***Abstract*—This letter extends the analysis of wave propagation in transmission lines with *LC*-parameters varying in space and time and the related effect of energy accumulation emerging from the concept of dynamic materials. We consider a practically important scenario of functionally graded checkerboard in space and time, i.e., the assembly combined of two dielectrics with material property transition zones applied instead of sharp interfaces. It is shown that the energy accumulation in traveling waves is preserved for certain ranges of material and geometric parameters.**

***Index Terms*—Capacitance, energy accumulation, inductance, spatial-temporal laminate, transmission line.**

I. Introduction

Selected effects that arise in wave propagation through spatial non-uniformities along with temporal variations have been considered, e.g., in [1]-[4]. These and other special phenomena emerging from space-time property variability have shaped a special concept of the so-called dynamic materials (DM) [5]-[7]. One of the DM effects is the energy accumulation in electromagnetic waves propagating in space- and time-varying transmission lines. An analysis and numerical simulation of this phenomenon were given in [5] and [8]. More specifically, in these papers, we studied wave propagation along the material structure that may be perceived in 1D space and time as a double periodic checkerboard. Such formation may be viewed as a periodic array assembled in space from two dielectrics differing in their properties [8]. This material arrangement also switches properties periodically in time. The interfaces between the two materials are therefore spatial and temporal; in [5] and [8], it has been assumed that spatial interfaces are sharp and temporal transitions are instantaneous.

In the present letter, we focus on some problems that should be addressed to facilitate material implementation of a DM checkerboard in practical transmission lines. In such lines, the lumped parameters (i.e., the inductance and capacitance) always change with certain degree of inertia. We consider a modified material arrangement that preserves all features of an ideal checkerboard [5], [8], but allows for non-sharp interfaces both in space and time, and releases the requirement of matching wave impedances. We introduce layers in which material properties exhibit a gradual linear transition between the values related to different uniform materials that occupy interiors of material cells, as shown in Fig. 1. Attention is mostly focused on the gradient in the wave velocity, while the impedance mismatch is illustrated only numerically. This work is specifically aimed to show that, despite such changes in the interfaces, the energy accumulation in traveling waves is still preserved; we particularly specify conditions necessary for such preservation.

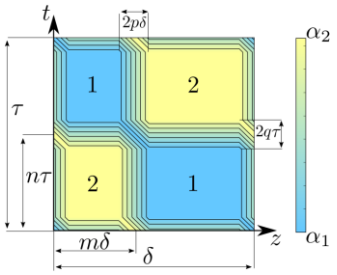

Fig. 1. Checkerboard with material property transitions zones (one spatial-temporal period).

II. Theoretical Background

In what follows, we use the concept of variable property materials in the context of wave propagation along transmission lines with variable parameters. In Fig. 1, the spatial period is δ, the spatial volume fraction is m, the temporal period is τ, and the temporal volume fraction is n; the wave velocity is shown to be in the range on the right. The width of each spatial transition region is $2p\delta$, and the width of temporal transition region is $2q\tau$. We term this formation a functionally graded (FG) checkerboard.

Following [5] and [8], we study energy transformation that accompanies waves traveling through such a transmission line. The wave $u(z, t)$ is governed by the following wave equation:

$$(Cu_t)_t - ((1/L)u_z)_z = 0,\ (z, t) \in [a, b] \times [0, T], \quad (1)$$

$$u(z, 0) = u_0(z),\ u_t(z, 0) = u_1(z)\ . \quad (2)$$

where $C(z, t)$ and $L(z, t)$ are, respectively, linear capacitance and inductance taking values C_1, L_1 in material 1, and C_2, L_2 in material 2. For simplicity, we disregard the boundary conditions and assume that the line is infinite. For our purposes it is

Manuscript received August 12, 2016.

K.A. Lurie, W.C. Sanguinet, S.L. Weekes, and V.V. Yakovlev are with the Department of Mathematical Sciences, Worcester Polytechnic Institute, Worcester, MA, 01609 USA (e-mail: klurie@wpi.edu; vadim@wpi.edu).

D. Onofrei is with the Department of Mathematics, University of Houston, Houston, TX, 77294 USA

This article has been accepted for publication in a future issue of this journal, but has not been fully edited. Content may change prior to final publication. Citation information: DOI 10.1109/LAWP.2016.2647205, IEEE Antennas and Wireless Propagation Letters

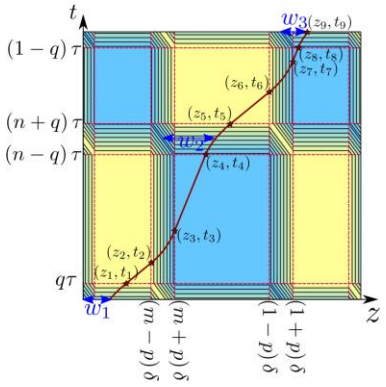

Fig. 2. Specific type of limit cycle studied.

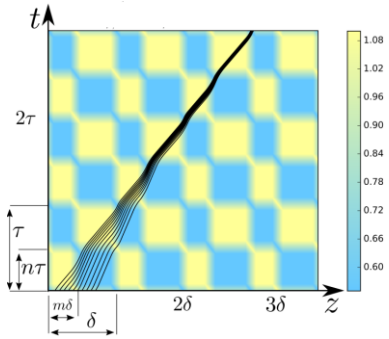

Fig. 3. FD checkerboard structure in space-time with wave routes for $\delta = 1.0$, $\tau = 1.0$, $m = 0.4$, $n = 0.5$, $\alpha_1 = 0.55$, $\alpha_2 = 1.1$, $p = 0.075$, and $q = 0.075$.

convenient to consider, instead of C and L, the phase velocity $\alpha = 1/\sqrt{LC}$ and wave impedance $\gamma = \sqrt{L/C}$ as material parameters; they take values α_1, γ_1 and α_2, γ_2 in materials 1 and 2, and it is assumed that $\alpha_2 > \alpha_1$.

We benefit from this choice because the phase velocity alone defines the pattern of wave routes in space-time. The paths of waves are given by solutions $z = z(t)$ of

$$z_t = \alpha(z(t), t), \quad z(t_0) = z_0. \tag{3}$$

Wave impedance is responsible for the assignment of energy to waves traveling in different directions prescribed by the wave routes. This means that such routes and energy distribution may be controlled independently by the phase velocity and wave impedance, respectively.

In [5] and [8], a checkerboard with sharp interfaces and matching wave impedances $\gamma_1 = \gamma_2 = \gamma$ was discussed. Two key effects observed in [5]-[7] were confirmed:

A. *Energy accumulation* occurs within some extended ranges of parameters m, n, α_1 and α_2, regardless the value of γ. These parameters are purposefully chosen to belong with certain domain; with such a choice, the wave routes enter the slow material 1 across the spatial interfaces, and leave them across the temporal ones. These wave trajectories are accompanied by energy accumulation at temporal transients and energy preservation at spatial crossings. This performance of wave trajectories guarantees the energy accumulation, and evades the energy loss.

B. Accumulated energy is *concentrated within a series of dense groups of wave routes* (one group per period). Each group converges to a selected wave route – a limit cycle, i.e., to a pulse that exhibits sharpening and carries progressively increasing power. There are two families of such cycles (pulses), one family traveling forward, and another backward; when $\gamma_1 = \gamma_2$, there is no energy exchange between them. A checkerboard demonstrating these properties is termed *ideal*.

The range of energy accumulation in pulses is given by the following set of inequalities [7], [8]:

$$\begin{aligned} \frac{\alpha_1 + \left(1 - \frac{\alpha_1}{\alpha_2}\right) m\beta - \beta}{\alpha_1 - \alpha_2} \le n \le \frac{\alpha_1 + \left(1 - \frac{\alpha_2}{\alpha_1}\right) m\beta - \beta}{\alpha_1 - \alpha_2} \\ \frac{m\beta - \alpha_2 + \frac{(1-m)\alpha_2\beta}{\alpha_1}}{\alpha_1 - \alpha_2} \le n \le \frac{m\beta - \alpha_2 + \frac{(1-m)\alpha_1\beta}{\alpha_2}}{\alpha_1 - \alpha_2} \end{aligned}, \tag{4}$$

with $\beta = \delta/\tau$. Notice that γ does not appear in (4). These inequalities are critical in a sense that violation of one of them may slow down the formation of pulses, but the energy accumulation may still be preserved, though probably not within well-developed pulses. Inequalities (4) secure the special performance of the wave routes indicated above in A. Particularly, they imply that inequalities

$$\alpha_1 \le \beta \le \alpha_2 \tag{5}$$

are necessary for energy accumulation.

III. Wave Propagation and Limit Cycles in FG Checkerboard

We now consider conditions for limit cycles for FG checkerboards, assuming for ease of analysis, that $\gamma_1 = \gamma_2 = \gamma$. Expressing C and L in (1) through α and γ and introducing the potential v, we replace (1) by the system

$$u_t - \gamma\alpha v_z = 0, \tag{6}$$

$$v_t - (\alpha/\gamma)u_z = 0. \tag{7}$$

We will produce inequalities similar to (3) taking into account the gradual transitions in properties illustrated in Fig. 1.

Fig. 2 shows a specific type of limit cycle considered in this paper; the class of routes is described earlier in A. We introduce a transition zone in which the phase velocity linearly changes (in space or time) from α_1 to α_2, and *vice versa*. As long as the limit cycle does not originate on a corner, we can choose parameters p and q that characterize the transitions widths small enough to guarantee that the wave routes do not go too close to the rectangular regions around the corners where both spatial and temporal variation occur.

In Fig. 3, we show a pattern of right going wave routes associated with a doubly periodic linear FG checkerboard. The paths are calculated by numerically solving (3) via the 4th order Runge-Kutta method. The figure shows that the focusing effect (the existence of limit cycles) can still be found in the linear FG case.

The first condition we place on the transition zones is that both spatial and temporal widths must be smaller than the minimum width in the checkerboard cells:

$$q < \frac{\min\{n, (1-n)\}}{2}, \quad p < \frac{\min\{m, (1-m)\}}{2}. \tag{8}$$

This article has been accepted for publication in a future issue of this journal, but has not been fully edited. Content may change prior to final publication. Citation information: DOI 10.1109/LAWP.2016.2647205, IEEE Antennas and Wireless Propagation Letters

TABLE I
COEFFICIENTS IN INEQUALITIES (13)

i	$<_i$	b_i	c_i	d_i	e_i
1	$>$	$-\frac{\beta\lambda}{\alpha_2}$	$\frac{2\beta\lambda(\lambda+1)(\lambda-\ln(\lambda)-1)}{\alpha_2(\lambda-1)^2}$	$\lambda+1$	$\frac{\lambda(\alpha_2-\beta)}{\alpha_2(\lambda-1)}$
2	$>$	$\frac{\beta}{\alpha_2}$	$\frac{2\beta(\lambda+1)(\lambda\ln(\lambda)-\lambda+1)}{\alpha_2(\lambda-1)^2}$	$\frac{\lambda+1}{\lambda}$	$\frac{\lambda(-\alpha_2+\beta)}{\alpha_2(\lambda-1)}$
3	$<$	$-\frac{\beta\lambda}{\alpha_2}$	$\frac{-2\beta\lambda(\lambda+1)(\lambda-\ln(\lambda)-1)}{\alpha_2(\lambda-1)^2}$	$-(\lambda+1)$	$\frac{-\alpha_2+\beta\lambda^2}{\alpha_2(\lambda-1)}$
4	$<$	$\frac{\beta}{\alpha_2}$	$\frac{-2\beta(\lambda+1)(\lambda\ln(\lambda)-\lambda+1)}{\alpha_2(\lambda-1)^2}$	$-\frac{\lambda+1}{\lambda}$	$\frac{\lambda(\alpha_2-\beta)}{\alpha_2(\lambda-1)}$

Based on these constraints, we define $\sigma = (1/2)\min\{m, (1-m), n, (1-n)\}$, and assume that the limit cycle starts in the first spatial period at $(z, t) = (z_1, 0)$:

$$p\delta < w_1 < z_1. \tag{9}$$

The wave then travels through the linear region to point (z_1, t_1), as shown in Fig. 2. The location of this point is given by integration of the equation of the wave route as

$$z_1 = w_1 + \left[\frac{1}{4}\alpha_1 + \frac{3}{4}\alpha_2\right] q\tau; \tag{10}$$

it must obey $w_1 < z_1 < m\delta - p\delta$. The limit cycle then travels through pure material 2 to (z_2, t_2) and then through a spatially linear region to the next intersection point (z_3, t_3). We have

$$t_2 = q\tau + \frac{1}{\alpha_2}(m\delta - p\delta - z_1), \tag{11}$$

and

$$t_3 = t_2 + \frac{2p\delta}{(\alpha_1 - \alpha_2)}\ln\left(\frac{\alpha_1}{\alpha_2}\right), \tag{12}$$

along with the requirement $qt < t_2 < t_3 < n\tau - q\tau$ as seen in Fig. 2. Continuing this procedure, we reach the point (z_9, t_9) and end up, after some algebraic manipulations, with four basic inequalities in m, n, p, and q:

$$n <_i b_i m + c_i p + d_i q + e_i,\ i = 1, 2, 3, 4, \tag{13}$$

with the coefficients given by Table 1, where $\lambda = \alpha_2/\alpha_1$.

These inequalities constitute the necessary and sufficient conditions for the formation of a limit cycle and therefore specify the admissible range of parameters. When $p = q = 0$ in (8), they reduce to (4). To make a limit cycle, we require that the value z_1 generates $w_1 = w_3$. As for an ideal checkerboard [8], there are two values of z_1, demonstrating this property: one value for a stable, another for unstable limit cycle. The cycles alternate; they begin on the z-axis in the fast (slow) materials for stable (unstable) limit cycles. The above analysis is for stable cycles.

Fig. 4 illustrates the (m, n) region that is satisfied by the inequalities (13). It also shows the basic restrictions on the property transition zones (namely, $p < \sigma$, $q < \sigma$). Each line labelled in the legend as l_i relates to the corresponding ith inequality (13). We see that the region is indeed bounded really by only the lines l_1, l_2, l_3, l_4 coming from the first four inequalities.

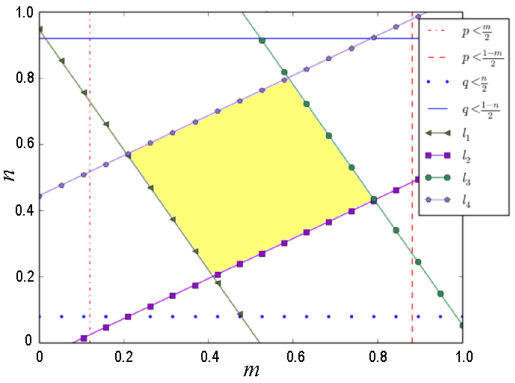

Fig. 4. The shaded region in the mn-space shows where the inequalities are satisfied for $\alpha_2 = 1.65$, $\lambda = 3.0$, $p = 0.06$, $q = 0.04$; the pairs of vertical and horizontal lines represent inequalities (8).

If p and q are small enough, e.g., $1 - 4p > 0$, $1 - 4q > 0$, and $\lambda > (1\text{-}p)/(1\text{-}2p)$, then inequalities (5) are replaced by

$$\alpha_1\left(\frac{1+2(\lambda-1)q}{1-\frac{4(\lambda-\ln(\lambda)-1)}{\lambda-1}p}\right) \le \beta \le \alpha_2\left(\frac{1-\frac{2(\lambda-1)}{\lambda}q}{1+\frac{4(\lambda\ln(\lambda)-\lambda+1)}{\lambda-1}p}\right). \tag{14}$$

This follows from inequalities 1-4 in Table I after some algebraic manipulations. When $p = q = 0$, inequalities (14) reduce to (5).

When we allow for γ_1 to be different from γ_2, the overall pattern of wave routes nevertheless remains the same. However, the energy carried by each wave is affected for two reasons. Firstly, this is the exchange of energy between families of right and left going waves, and, secondly, possibly because of the loss of energy to the external agent caused by waves entering the slower materials via the temporal interface [5]. We now consider energy accumulation in a linear FG checkerboard structure.

IV. ENERGY ACCUMULATION IN FG CHECKERBOARD

We numerically calculate the energy accumulated in a FG checkerboard with C and L treated as material parameters. The total energy at time t of a wave located within a segment $z \in (a, b)$ can be expressed, following [9], as:

$$E(t) = \int_a^b \left(C(z,t)u_t^2 + \frac{1}{L(z,t)}u_z^2\right) dz \tag{15}$$

In order to evaluate the evolution of energy over time the integral (15) is computed at a series of discrete time steps Δt. If the material parameters allow for stable limit cycles, we expect the solution of system (6)-(7) to develop from the initial state at $t = 0$ into a series of sharpening pulses. That is, regions with high gradient of u will take shape as time goes on. In order to accurately capture these regions of rapid transitions, we use adaptive mesh refinement such that the grid is fine in regions where u_z is high and coarser when u is smoother. The integral (15) requires evaluating the time derivatives at any given point, but this is challenging with an adaptive mesh that changes in time. Instead, we rewrite the energy formula with only spatial derivatives using (6):

This article has been accepted for publication in a future issue of this journal, but has not been fully edited. Content may change prior to final publication. Citation information: DOI 10.1109/LAWP.2016.2647205, IEEE Antennas and Wireless Propagation Letters

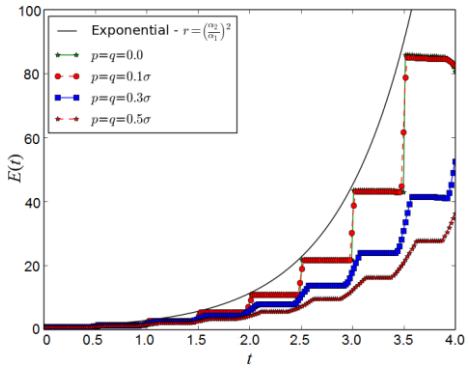

Fig. 5. Energy evolution for various values of smoothing parameters p and q (a = 0, b = 4).

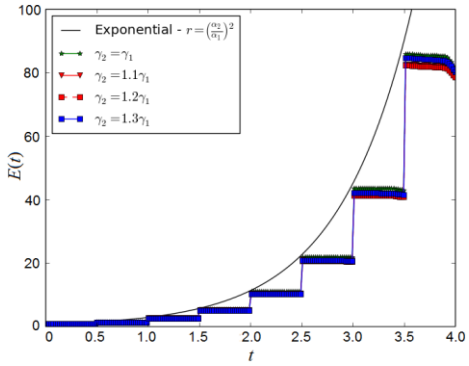

Fig. 6. Energy evolution for mismatch in the values of wave impedance γ (a = 0, b = 4).

$$E(t)=\int_a^b\left(\frac{1}{C(z,t)}v_z^2+\frac{1}{L(z,t)}u_z^2\right)dz \quad . \tag{16}$$

We compare the computed energy with the energy increase first theorized in [5] and observed in [6] and [8] for the case when $\gamma_2 = \gamma_1$, which gives an increase after every temporal period by a factor $(\alpha_2/\alpha_1)^2$.

Fig. 5 characterizes energy evolution for several pairs of values of p and q that depict the functional grading; we assume that there is no wave impedance mismatch. However, if $p = q \le 0.5\sigma$, then the energy accumulation persists, but becomes less intensive than in the case of sharp interfaces. The reason is that, unlike the impedance mismatch, the functional grading affects the wave routes and may slow down and even decrease the energy accumulation.

Now we assume that both spatial and temporal interfaces are sharp, but allow for a mismatch in wave impedance. In Fig. 6, for the ratio γ_2/γ_1 taking values from 1 to 1.3, we see that the energy accumulation is practically independent of impedance mismatch. The pattern of wave routes remains unaffected, but due to wave reflection at material property interfaces, the energy does not concentrate in pulses as quickly as it does in the absence of reflections. However, the net energy is still accumulated at temporal transients from the slow materials to fast, but this time in the waves traveling in both directions. Concentration of energy in sharp pulses takes in these circumstances more time than in the absence of the wave impedance mismatch.

The case of impedance mismatch is of a special interest due to a number of reasons. Firstly, the energy is then redistributed between families of left- and right-going waves. Secondly, the wave reflections slow down the energy concentration in pulses. Thirdly, the energy loss may be possible at temporal transients from fast materials into slow. Fourthly, the wave impedance mismatch makes the system capable of producing resonances due to wave reflections. The general analysis of all these factors requires special effort with final results that are hard to predict. An evidence for that is given by Fig. 6 where practically no effect in the *net* energy accumulation is observed for relatively large mismatch γ_2/γ_1 = 1.3. This observation may be viewed as an advantage of wave impedance mismatch compared to that in wave velocity.

The solid curve in Figs. 5 and 6 passes through points representing the exponential energy growth at moments of temporal switching, with the rate defined as $\ln(\alpha_2/\alpha_1)^2$. Energy is accumulated at selected moments of temporal switching; between two such moments it remains constant.

V. Conclusion

This letter continues investigation of the energy/power accumulation developed in a transmission line with space- and time-dependent parameters represented in [8] as the material DM checkerboard structure. In that paper, we considered an ideal assembly in which the temporal and spatial material interfaces between adjacent cells were sharp, and the wave impedances of different materials matched. In the present letter, we have examined the influence of gradual spatial and temporal transitions from one material cell to another. It has been found that the energy accumulation persists for certain ranges of parameters that characterize deviations from an ideal assembly. Both theoretical and numerical evidence for such persistence have been demonstrated. The case of wave impedance mismatch deserves additional, more detailed study because of many counteracting effects. The presented results may facilitate the engineering work towards fabrication of the transmission lines employing the proposed mechanism of energy accumulation.

References

[1] M.M. Idemen, *Discontinuities in the Electromagnetic Field*, Wiley-IEEE Press, 2011.

[2] M.A. Salem and C. Caloz, "Space-time cross-mapping and application to wave scattering," *arXiv:1504.02012*, May 2015.

[3] A. Scott, *Active and Nonlinear Wave Propagation in Electronics*, Wiley-Interscience, 1970.

[4] N.A. Estep, D.L. Sounas, J. Soric, and A. Alù, "Magnetic-free non-reciprocity and isolation based on parametrically modulated coupled-resonator loops," *Nature Physics*, vol. 10, no 12, pp. 923-927, 2014.

[5] K.A. Lurie and S.L. Weekes, "Wave propagation and energy exchange in a spatio-temporal material composite with rectangular micro-structure," *J. Mathem. Analysis & Applications*, vol. 314, pp. 286–310, 2006.

[6] K.A. Lurie, *An Introduction to the Mathematical Theory of Dynamic Materials*, Springer, 2007.

[7] K.A. Lurie, D. Onofrei, and S.L. Weekes, "Mathematical analysis of the energy concentration in waves travelling through a rectangular material structure in space-time," *J. Mathem. Analysis and Applications*, vol. 355, pp. 180-194, 2009.

[8] K.A. Lurie and V.V. Yakovlev, "Energy accumulation in waves propagating in space- and time-varying transmission lines," *IEEE Antennas & Wireless Propag. Letters*, vol. 15, pp. 1681-1684, 2016.

[9] J.D. Jackson, *Classical Electrodynamics*, John Wiley & Sons, 1962.